COMMUNICATIONS

Magnetic Resonance in Medicine 43:163–169 (2000)

In Vivo MR Micro Imaging With Conventional Radiofrequency Coils Cooled to 77°K

Alexander C. Wright,* Hee Kwon Song, and Felix W. Wehrli

Cryogenically cooled conventional surface coils are shown to provide significant signal-to-noise ratio (SNR) gains for MR micro imaging of tissue structure in vivo. Measurements are described which employ a simple, all-polyvinyl chloride (PVC) vacuum dewar capable of maintaining a bath of liquid nitrogen around the coil, within 5 mm of the tissue to be imaged. Images acquired in vivo at 64 MHz with a 2-cm diameter copper coil cooled to 77 K demonstrated a gain in SNR of approximately 2.7 ± 0.3 relative to those obtained with the same coil at room temperature under otherwise identical conditions. This increase is consistent with the reduction in coil resistance and the minor contribution to overall resistance from the imaging object. The performance of the coil is illustrated with images from the human finger and rabbit eye and potential applications are discussed. Magn Reson Med 43:163–169, 2000. © 2000 Wiley-Liss, Inc.

Key words: in vivo; MR microscopy; cryogenic cooling; RF coils; SNR improvements

Scan time to achieve a given SNR scales as the inverse sixth power of linear resolution (1). SNR is thus the most significant limitation to achieving higher resolution in MRI. To improve SNR, thermal noise voltages received from the sample can be reduced using small surface and implanted RF coils, and noise voltages intrinsic to the receive coil can be minimized by lowering coil resistance and coil temperature. This intrinsic contribution is significant at resonance frequencies corresponding to ^{1}H imaging at 1.5–4.0 T for coils or samples ≤ 2 cm diameter, in which case resistive RF losses in the coil surpass inductive and dielectric losses in the sample. Under these conditions cryogenic cooling of the coil is most effective in improving SNR.

At liquid nitrogen temperature (77 K), the quality factor (Q) of normal metal (copper, silver, etc.) coils increases 2–3 times and that of high-T_C superconductor (HTS) coils two or three orders of magnitude more, suggesting large potential gains in SNR for non-loading samples (SNR $\propto \sqrt{Q}$). Minor sample loading at room temperature reduces the gains in SNR since the sample becomes the dominant source of resistance at low temperature. In this regime, as the following example demonstrates, the SNR gains achievable with conventional metal coils may approach those of superconducting because once the sample-dominated limit has been reached, further increases in Q have little effect. Suppose a coil is loaded by a sample such that its room temperature (300 K) Q drops by 10%. In this case, the SNR gain for a copper coil upon cooling from 300 to 77 K is projected to be 2.34, whereas an identical HTS coil with a 100-times-higher Q would provide a gain of 3.06, one with a Q approaching infinity 3.16. Thus 75% of the available gain is already achieved with the copper coil.

SNR improvements with a cryo-cooled NMR probe designed for ^{13}C NMR spectroscopy at 45.9 MHz of room-temperature samples were first demonstrated by Styles, et al. (2). Subsequently, SNR gains have been observed with large coils in low-field MRI systems, but the greatest gains are expected with small coils since sample noise voltage scales roughly as frequency × (diameter)$^{3/2}$ (3). Cooling a 20-cm square copper surface coil designed for whole-body imaging at low field strength (0.15 T) with liquid nitrogen, Hall, et al. achieved a factor of 1.3 improvement in SNR for in vivo images of the human lumbar spine (4). Okada, et al., using a 30-cm square HTS coil cooled in liquid nitrogen, reported SNR gains of 1.6 in the human thoracic spine at 0.064 T (5). SNR gains observed with smaller coils at several field strengths showing considerable variability may be due to differences in the performance of HTS materials as well as in the extent to which the coil is loaded by the sample. For example, Van Heteren, et al., using a 6-cm diameter HTS coil cooled to 77 K, obtained in vivo images of the human eye at 0.064 T with SNR gains of 1.7 over a room temperature copper coil (6). Vester, et al., cooled a 3.4-cm diameter HTS coil in liquid nitrogen and obtained in vivo images of the human wrist at 0.2 T with SNR gains of 4 to 9.5, depending on sample loading, compared to a similar silver-plated copper coil at room temperature (7). At high field (7 T), Black, et al., demonstrated a factor of 10 improvement in SNR for MR microscopy of very small room temperature samples by using a 2-cm diameter HTS coil cooled to 10 K (8). In addition, Miller, et al. (9) recently achieved a nearly fourfold SNR gain at 2 T for in vivo imaging of rat brain using a 2-cm diameter HTS coil cooled to 30 K, compared to a warm copper coil. The latter result is particularly promising for cryo-cooled coil applications to in vivo MR microscopy of animals and, possibly, in humans at medium field strengths.

The purpose of the present work was to determine the gains achievable for in vivo MR microscopy by cooling small circular copper surface coils, which have several advantages in terms of simplicity, stability and cost when compared to HTS coils. The results presented here involve design and construction of a simple, cost-effective and

Department of Radiology, Hospital of the University of Pennsylvania, Philadelphia, Pennsylvania.

*Correspondence to: Alexander C. Wright, Ph.D., Department of Radiology, 1 Silverstein, Hospital of the University of Pennsylvania, 3400 Spruce Street, Philadelphia, PA 19104. E-mail: wright@oasis.rad.upenn.edu

Received 12 April 1999; revised 11 June 1999; accepted 15 June 1999.

easy-to-use liquid nitrogen vacuum dewar utilizing conventional coil technology for micro imaging at 1.5 T. The methodology thus offers an alternative to HTS or implanted coils, with a wide range of imaging applications in vivo.

THEORY

Lowering coil temperature effectively reduces the mean square thermal voltage fluctuations (Johnson noise) of the charge carriers in the conducting material, and thus may increase SNR. In the case considered here, separate, mutually decoupled coils are used for transmission and reception. Further, the receive coil is used in the same position relative to the sample for room temperature and cryogenic measurements. This means that exactly the same sample magnetization is detected by the coil, whether the receive coil is warm or cold. Hence the cryogenic SNR gain can be evaluated simply by the warm-to-cold ratio of the thermal noise.

The Nyquist formula (10) states that the mean square of the noise voltage fluctuations in a conductor is proportional to the product of its absolute temperature T and its (frequency-dependent) resistance R:

$$\langle V\rangle^2 = 4k_B TR\Delta f \qquad [1]$$

where k_B is Boltzmann's constant and Δf is the frequency bandwidth of the measurement. The total mean square noise voltages seen by the receiver can be expressed as a sum of uncorrelated contributions from the preamp, coil and sample (11), i.e.,

$$\langle V_{\text{Total}}\rangle^2 = \langle V_{\text{preamp}}\rangle^2 + \langle V_{\text{Coil}}\rangle^2 + \langle V_{\text{Sample}}\rangle^2 \qquad [2]$$

Furthermore, recognizing that resistances, which add in series for coil and sample, are inversely related to quality factors ($Q = \omega_0 L/R$), one can write

$$Q^{-1}_{\text{Loaded}} = Q^{-1}_{\text{Unloaded}} + Q^{-1}_{\text{Sample}} \qquad [3]$$

Assuming that preamp noise voltages are negligible compared to those of the coil and the sample (an assumption justified at the typical preamplifier noise figures of 0.3 dB), the SNR ratio (gain) at the two temperatures (77 and 300 K) can then be written as

$$\frac{SNR_{77}}{SNR_{300}} = \sqrt{\frac{300\cdot Q^{-1}_{\text{Unloaded},300} + 300\cdot Q^{-1}_{\text{Sample}}}{77\cdot Q^{-1}_{\text{Unloaded},77} + 300\cdot Q^{-1}_{\text{Sample}}}} \qquad [4]$$

Equation [4] simply entails a measurement of the coil's room temperature Q when loaded with the sample and its unloaded Q at room and cryogenic temperature. For example, a coil with unloaded Q's of 100 at room temperature (300 K) and 200 in liquid nitrogen (77 K) and a loaded room temperature Q of 90 (10% loading) would produce a cryogenic SNR gain factor of 2.2.

To obtain an analytic estimate of SNR gain for cold coils as a function of coil radius and field strength, frequency-dependent expressions of coil and sample resistances can be derived for simple geometries. From these, it is also useful to predict the ratio of loaded to unloaded Q:

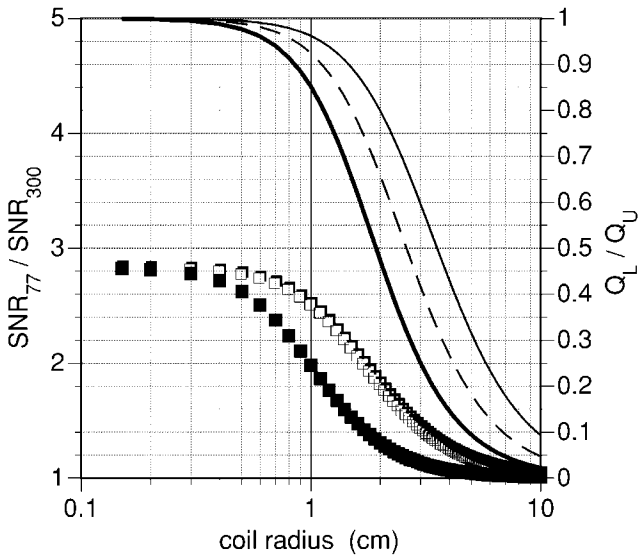

FIG. 1. Loaded to unloaded Q ratio versus coil radius for two magnetic field strengths (thin line = 1.5 T; thick line = 4 T), both at room temperature, and for 1.5 T at 77 K (dashed line). Also shown are SNR gain factors at 1.5 T (white squares) and 4 T (black squares) expected upon cooling the coil in liquid nitrogen (77 K). Assumed coil geometry was 3 mm O.D. copper tubing made into circular coils, and assumed sample geometry was a semi-infinite half-space of homogeneous conductivity 6 mm from the coil.

$$\frac{Q_L}{Q_U} = \frac{R_{\text{Coil}}}{R_{\text{Coil}} + R_{\text{Sample}}} \qquad [5]$$

The expression for R_{Sample} adopted here assumes an infinite homogeneous half-space at distance d from the plane of the coil (12):

$$R_{\text{Sample}} = \frac{2}{3\pi}\,\mu_0^2\omega_0^2\sigma a^3 \tan^{-1}\left(\frac{\pi}{8}\cdot\frac{a}{d}\right) \qquad [6]$$

where a is the coil radius and ω_0 is angular frequency. The value for the sample conductivity σ was adjusted to force agreement between measured and calculated values of Q_L/Q_U for the coil used here when loaded by a human finger. This effective conductivity was 0.17 S/m. R_{Coil} was approximated using the frequency-dependent skin depth δ_{Cu} and the resistivity ρ_{Cu} of copper at each temperature (13) to obtain an effective cross-sectional area for the current path in a coil made from hollow tubing of outer diameter D:

$$R_{\text{Coil}} = \frac{2a\rho_{\text{Cu}}}{(\frac{1}{2}D)^2 - (\frac{1}{2}D - \delta_{Cu})^2} \qquad [7]$$

where

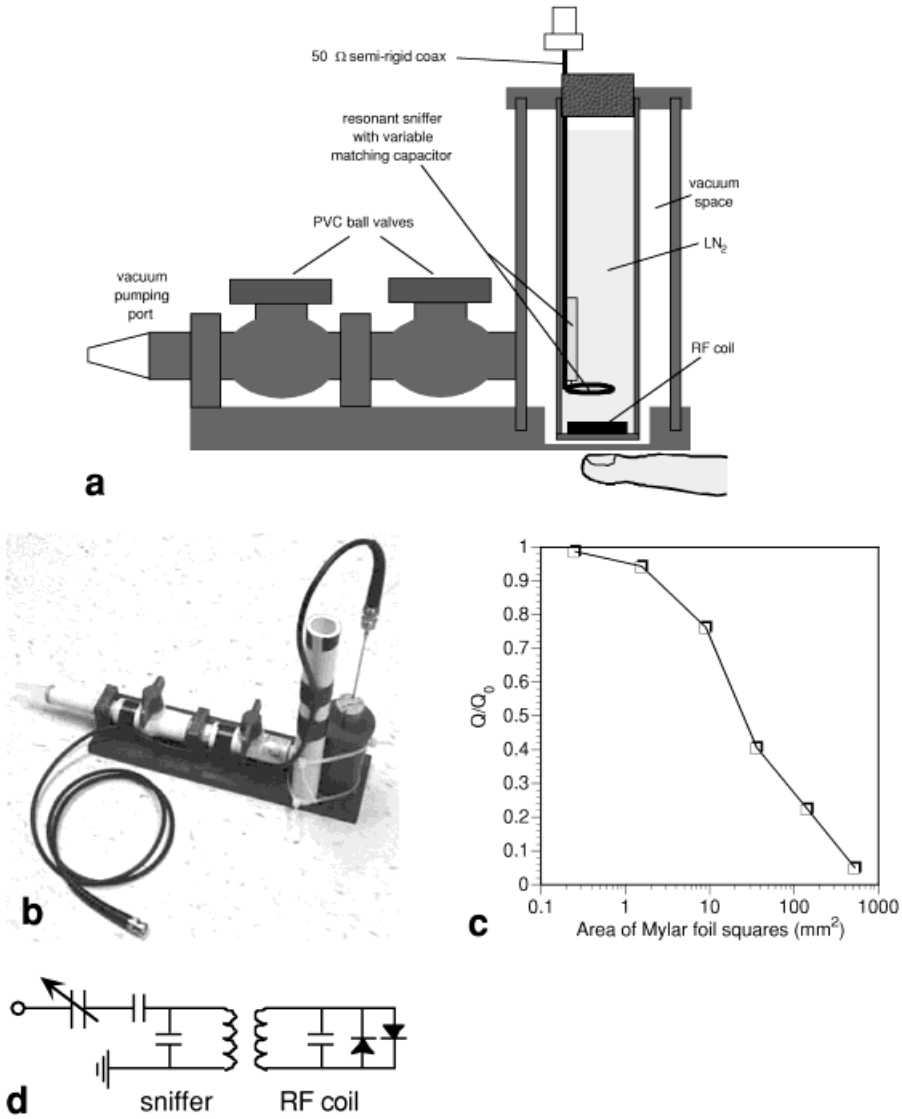

FIG. 2. **a–b:** All-PVC dewar for liquid nitrogen, showing relative location of finger. **c:** Q values (at room temperature) of the copper RF coil placed on a 1/16 inch thick plastic sheet covered on the opposite side with sectioned Mylar film, for different areas of the (contiguous) Mylar sections. Q values are normalized to the Q value of the coil in free space. **d:** Circuit diagram shows tuning/matching scheme for coil + sniffer as well as transmit decoupling strategy for the receive-only coil.

$$\delta_{Cu} = \sqrt{\frac{2\rho_{Cu}}{\mu_0\omega_0}} \quad [8]$$

Equations [4] and [5] are plotted versus coil radius in Fig. 1 at 1.5 T and 4.0 T field strength, showing that SNR gains greater than 2 are predicted at 1.5 T for coil radii 1 cm or less, where loading is below 10%.

MATERIALS AND METHODS

Dewar Design

A small, easily positioned vacuum dewar was designed to maintain a 30-cm^3 bath of liquid nitrogen (LN_2), topped with a cork stopper (Fig. 2a–b). Dewar walls and valves were constructed entirely of PVC plastic. High-vacuum ($< 10^{-5}$ torr) was achieved by roughing and oil diffusion pumps, which were disconnected from the dewar prior to its placement in the scanner. Silicone high-vacuum grease (Dow Corning, Inc.) was applied to external surfaces of the PVC ball valves to improve the vacuum seal. Vacuum space surfaces were lined with aluminized Mylar film, sectioned to minimize loading effects. A low-emissivity surface is standard practice in cryogenic engineering for reducing radiative heat losses and metallized film is readily available for this purpose (e.g., Kellogg's Pop-Tarts wrappers). However, in MR applications such as considered here, induced eddy current losses in the film can cause strong loading of the RF coil. This problem, analogous to the loading effect in tissues, can effectively be eliminated by sectioning the film into small regions so as to break eddy current paths. Losses in the film were characterized at room temperature by measuring Q change for the coil resting on a 1/16-inch thick plastic sheet covered on the opposite side with sectioned Mylar film, for different areas of the (contiguous) Mylar sections (Fig. 2c). The coil Q, normalized to its unloaded value Q_0, decreases as the area of film sections increases. Clearly, losses are negligible for film section areas of about 1 mm^2. The curve would be expected to shift to the left at lower coil temperatures, but this would cause negligible additional losses for the film sectioning (1 mm^2) and coil used here.

Coil Design and Measurements

The receive coil used was a 17-mm diameter loop of 3-mm outer diameter (O.D.) copper tube resonated with a chip capacitor and decoupled from the body coil transmission by a parallel chip crossed diode. Effectiveness of the decoupling was confirmed by showing that identical RF transmitted powers were needed for a 90° pulse when imaging a phantom with the cold coil (77 K) and the same phantom and coil at room temperature, even though the respective Q's were quite different. Furthermore, images of a phantom (a 60-cm^3 syringe filled with copper sulfate-doped water), were free from artifacts that can occur if a receive coil couples power from the transmit coil. A resonant "sniffer" loop (14) inductively tuned and matched the receive coil to the external preamp (Fig. 2d). Thus both the receive coil and sniffer were immersed in the cryogen. The sniffer consisted of a 10-mm diameter loop of copper wire (1.5 mm thick), resonated by a chip capacitor and attached to a short length of semi-rigid 50 Ω coaxial transmission line. The transmission line was supported by a cork stopper and attached to a longer length of flexible 50 Ω coaxial cable connected to the MRI scanner preamp or to a Hewlett-Packard 8247B network analyzer for measuring reflected power. After calibrating for cable impedances, the coil was first tuned to 63.875 MHz (the carrier frequency of the 1.5-T scanner) by adjusting the height of the sniffer above the coil (12 mm). It was then matched to 50 Ω real by adjusting a variable capacitor in series with the sniffer. The gap between the coil and the external dewar surface was 4.8 mm, and 6 mm between the coil and the fingernail (d = 6 mm). A thin (1 mm) Styrofoam plate was fixed to the bottom dewar surface to provide additional insulation.

Q's were based on the –3 dB bandwidth of the transmission response. Transmission measurements were made with the network analyzer and two small nonresonant coupling loops held at appropriate distances and angles relative to the coil in order to avoid loading of the coil (Q damping) and to generate a symmetric response. The coil was first tuned and matched using the sniffer as described above and then Q values for the coil at room temperature (300 K) and immersed in LN_2 (77 K) were acquired for unloaded conditions and when loaded by a human finger in vivo. The measured Q values of the receive coil + sniffer combination, tuned and matched to 50 Ω at each temperature, were $Q_{U,77} = 260$ and $Q_{L,77} = 250$ at 77 K, and $Q_{U,300} = 125$ and $Q_{L,300} \approx 125$ at room temperature. The room temperature Q change upon loading (2%) was at the sensitivity limit of the measurement method, but the change measured at 77 K implies $Q_S \approx 6{,}500$ and $Q_{L,300} = 123$ (Eq. [3]), and a projected SNR gain of 2.7 (Eq. [4]). Clearly, the coil is negligibly loaded by a finger in spite of the proximity of the coil to the target. Even when the tuned and matched coil + sniffer combination was removed from the dewar and positioned adjacent to the finger (d = 0), the Q decrease at room temperature was only 2–3%.

Imaging Experiments and Analysis

To illustrate the potential of the coil for in vivo measurements, micro images of the human terminal phalanx of the right middle finger and of a rabbit's eye were obtained on a GE Medical Systems Signa 1.5-T whole-body scanner. The scanner was equipped with Echo Speed gradients (22 mT/m peak amplitude) and software version 5.6. The pulse sequence was a 3-D gradient echo utilizing a variable echo time (TE) as a means to enhance structures with short inherent T_2 such as the dermal layer under the nail (15). The following parameters were employed for the acquisition of both human and rabbit images: repetition time = 80 msec, $TE_{min} \approx 5.7$ ms, 30° flip angle, receive bandwidth = ±8 kHz, 512 × 512 matrix, frequency encoding in the anterior-posterior direction, 16 slices of 1 mm thickness, obtained in 11-min. scan time. Human images were acquired with a 4-cm field of view (78 × 78 μm^2 in-plane resolution) and rabbit images with a 6-cm FOV (117 × 117 μm^2). A standard, fixed-TE 3-D gradient echo sequence with these parameters would provide a minimum TE of 10.9 msec, but by using the strategies described in Ref. 15, the effective TE was reduced by 5.2 msec.

Experiments were performed with the coil in the dewar, first at room temperature, matched to 50 Ω. Then the coil and dewar assembly was removed from the scanner and the dewar was filled with LN_2. The coil (at 77 K) was again matched to 50 Ω and the dewar, with LN_2, was repositioned in the scanner. Each time, an axial reference scan was first performed, followed by the 3-D gradient-echo sequence with slice selection gradients along the right-left axis (sagittal views). Human imaging was performed with the subject lying prone with the right arm extended above the head. The middle finger of the right hand, palm down, was positioned under the dewar at the location of the coil. Small ridges on the underside of the dewar marked the coil and assured positioning repeatability. Rabbit imaging was performed on a New Zealand White male rabbit that had been anesthetized by intramuscular injection of a ketamine/xylazine cocktail, followed by a subcutaneous injection of urethane. Procedures had been approved by the institutional animal care and use committee. Eye movement under anesthesia was minimal, precluding the need for motion correction techniques. A lipid-rich ointment was applied to the corneal surface after the rabbit was sedated to maintain the cornea moist (visible in the images).

Magnitude images were reconstructed and analyzed using locally written IDL analysis tools (Research Systems, Inc., Boulder, CO). SNR was measured from mean pixel intensities in rectangular ROIs drawn on the tissue and drawn on the background. The regions enclosed at least 400 pixels in the tissue and at least 3000 background pixels.

RESULTS

Dewar Performance

Vacuum integrity was found to be critical to the effectiveness of the thermal insulation. Immediately after the dewar had been evacuated, the vacuum was sufficient to provide thermal insulation so that the external surface at the coil location became only slightly cool to the touch when the dewar was filled with LN_2. The additional 1-mm layer of Styrofoam, though not essential, resulted in a room temperature surface. After 48 hours, however, the

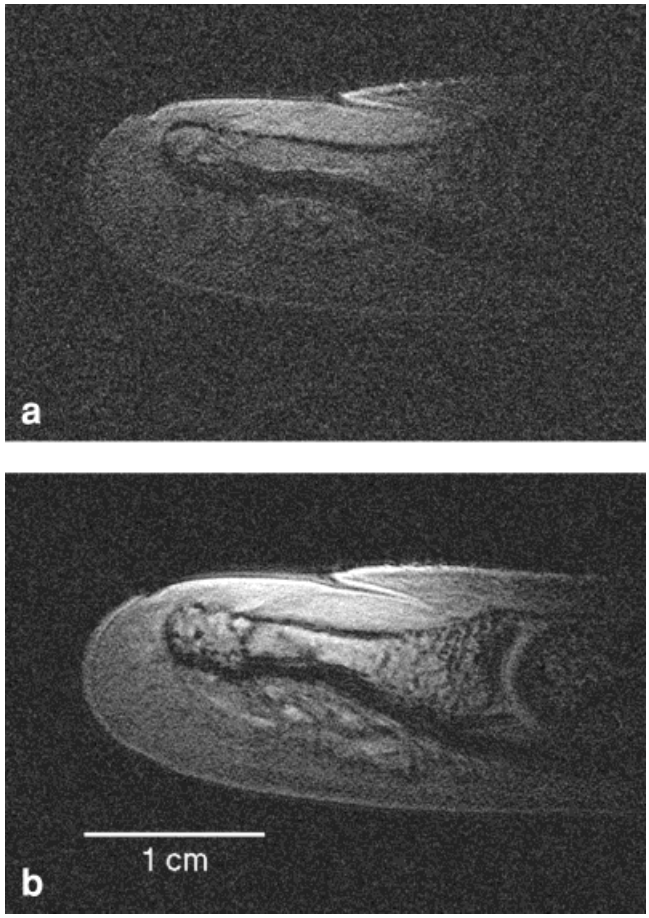

FIG. 3. In vivo MR micro images of the terminal phalanx of the right middle finger, obtained with a 3-D variable-TE gradient-echo pulse sequence in 11 minutes using a 2-cm diameter circular copper surface coil (78 × 78 × 1000 μm^3 voxel size): (**a**) at room temperature, (**b**) at 77 K. Both images were acquired with identical positioning and protocols.

vacuum degraded due to slow leakage through the PVC ball-valves, resulting in some condensation on the external dewar surface at the coil location when filled with LN_2. For the initial vacuum, LN_2 boil-off was estimated at 1.0 cm^3/min, which allowed 20 minutes of operation before a refill.

Phantom Imaging

Images of a 10-cm^3 syringe (1.5 cm diameter) filled with distilled water demonstrated an SNR gain factor of about 2.8, using rectangular regions drawn on the syringe cross-section and on the background (data not shown). As the loading from such a phantom is minimal, the SNR gain can be predicted by Eq. [4] assuming negligible losses in the sample ($1/Q_S \approx 0$). This gives a predicted gain of slightly more than 2.8, in excellent agreement with the measurements.

In Vivo Imaging

In vivo MR micro images of the same terminal phalanx of the right middle finger are shown in Fig. 3 for scans obtained with a) a room temperature coil and b) the same coil at 77 K with identical positioning and protocols (voxel = 78 × 78 × 1000 μm^3). SNR increased 2.4–3.0 times in the dermis under the nail, similar to the value of 2.7 predicted from Eq. [4] based on Q changes due to loading and cooling. The range represents the variation of values using slightly different sizes and locations of rectangular regions

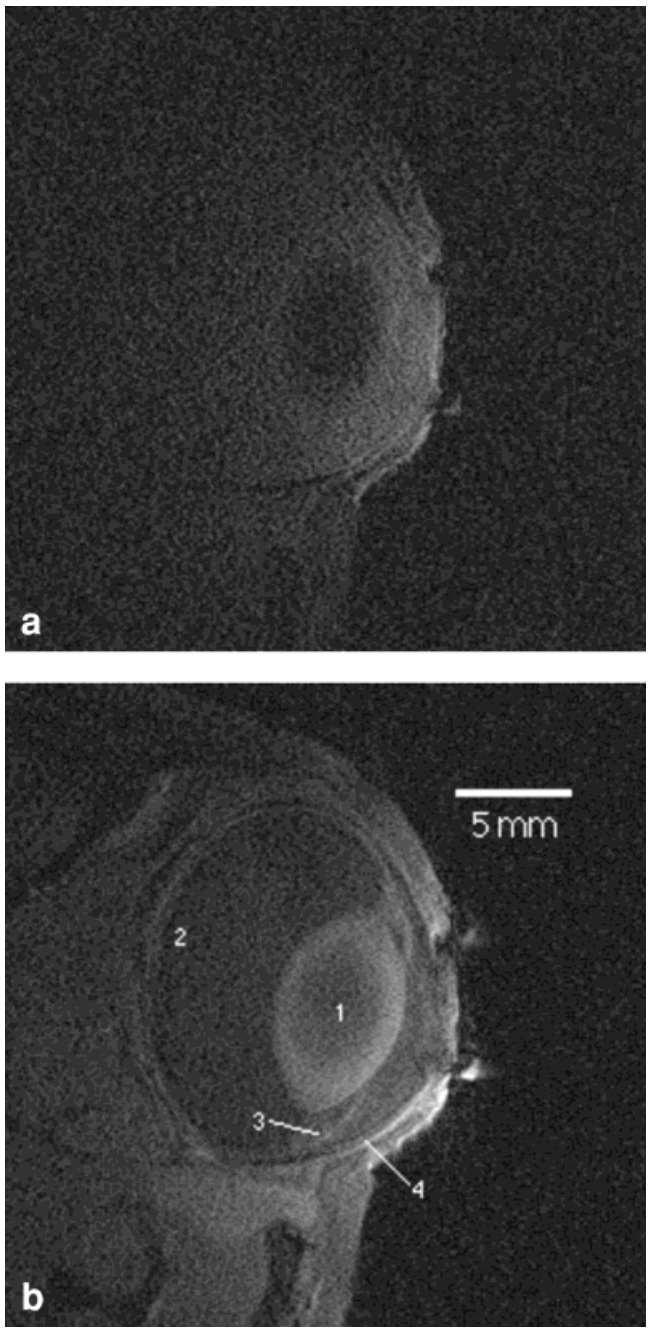

FIG. 4. In vivo MR micro images of the right eye of a rabbit (New Zealand White) obtained at 1.5 T with a 2-cm diameter copper coil, with imaging parameters equal to those of Fig. 3 except for a larger (6 cm) FOV (117 × 117 × 1000 μm^3 voxel size): (**a**) at room temperature (**b**) at 77 K, using identical positioning and protocols. Depending on location, SNR was increased by a factor of 2–2.5 in **b**. Numbered in **b**: 1, lens; 2, retina/choroid and sclera; 3, ciliary body and iris; 4, cornea.

in the dermis and is taken from two separate sets of warm/cold images. Epidermis, bone trabeculae and hypodermal structures of the pulp clearly are better visualized using the cryogenic coil compared to the same coil at 300 K.

The rabbit eye was chosen to demonstrate the potential of cryogenic coils as an ophthalmologic imaging tool where the field of view required is very small but resolution requirements are very stringent (16) (Figs. 4a and b). Visible in these images are the iris, the ciliary body, the lens, the cornea and the layers of retina/choroid and sclera at the back of the eye. Improvement in SNR was 1.7–2.2 in the aqueous humor and 2.5 in the anterior aspect of the lens. The gain measured in these images was slightly less than that seen for the finger, consistent with greater loading of the coil by the rabbit's eye and head. The loaded Q at room temperature was 110 (12% loading), corresponding to a predicted SNR gain of 2.1 upon cooling to 77 K.

DISCUSSION

This study has demonstrated that by cooling a small conventional copper surface coil with liquid nitrogen, SNR gains of about 2.7 are achievable for MR micro imaging of submillimeter anatomical structures in vivo. Very high-resolution images were obtained from superficial structures in humans and rabbits suggesting the method to be applicable to a wide range of problems requiring detailed knowledge of tissue microstructure.

The cryo-coil assembly and PVC vacuum dewar were designed for ease of use and low-cost operation. Details of size and shape can be tailored to specific requirements. The silicone grease applied to the PVC ball valves markedly enhanced the vacuum integrity and longevity. However, a high-vacuum valve can be used which would provide a better seal and longer-lasting vacuum. Furthermore, a larger LN_2 capacity would permit longer scans without the need to replenish the cryogen. While the dewar used here is primitive and merely serves as proof of principle, cryostats having thinner walls can be constructed using stronger materials such as G10 plastic (9) or thin ceramic plate (7). Use of a cold head (9,17) would permit the coil to be positioned closer to the sample by eliminating the need for an inner dewar wall. Such designs would allow greater proximity of the coil to the tissue, important for very small coils.

The coil tuning/matching inductive coupling scheme employed here was found to be effective and the technique can be adapted for use with HTS coils. A separate transmit (body) coil, as opposed to a surface coil for transmission and reception, provides a uniform tip angle over the entire field of view. Although in the present experiments a gradient echo sequence was used, tip angle uniformity would be especially important for spin echo imaging. In addition, if very high Q coils were used, there would be no limitations from long ring-down time or radiation damping, assuming adequate transmit/receive decoupling. During reception, the body coil was actively de-tuned, preventing resonant transfer of its noise to the receive coil. The receive coil used here was constructed from 3-mm O.D. copper tubing, having an isolated room temperature Q of 190. Higher Q coils may be pattern-etched on double-sided copper film with a Teflon substrate providing dielectric capacitance for self-resonance and eliminating the need for ceramic chip capacitors (18).

In general, sample loading is less of a problem at field strengths lower than 1.5 T, but at 4 T it reduces SNR gains (Fig. 1). Still, there are likely to be gains for small coils at 4 T, a field strength more typical of small animal imaging, particularly for imaging and spectroscopy of low-gamma nuclei since the loading is frequency dependent. Possible candidates are ^{23}Na (19) and ^{13}C (20) whose resonance frequencies are almost a factor of 4 lower than that of protons. Furthermore, at even lower temperatures (e.g., 10 K), additional SNR gains (over 5 times) may be possible for imaging the finger, where the loading is only 2% at 1.5 T with the copper coil used here. Although such temperatures are more difficult to achieve, the technology is not prohibitive.

Potential applications of cryocoils in humans comprise the noninvasive assessment of skin morphology and function, currently performed with high-frequency ultrasound, which provides poor contrast and is not amenable to the skin's deeper layers. A case in point is the delineation of pathologic structures such as glomus tumors and mucoid cysts of the nail apparatus (21), but the technology should be applicable to the staging of skin tumors in general (22). For specifically imaging the finger, a volume solenoid (23) or birdcage (24) coil would be expected to provide greater SNR than a surface coil, and these could be cooled similarly in a dewar without a great deal of added complexity. Another promising field is ophthalmology where noninvasive imaging techniques of sufficient resolution for pre- and postsurgical evaluation are lacking. The potential is perhaps even greater in small-animal imaging. This includes the study of progression and regression of atherosclerotic disease, which requires a detailed assessment of plaque morphology and content (25). Other anticipated applications involve the assessment of trabecular bone microstructure in studies where animals are followed longitudinally in response to treatment.

Finally, quantitative analyses of MR micro images in general are particularly likely to benefit from SNR gains through cryo-cooled coils. An example of considerable clinical interest is imaging and analysis of trabecular bone, currently possible at a resolution of $137 \times 137 \times 500\ \mu m^3$ in the human wrist. While the method has been shown to allow extraction of bone volume fraction (BVF) and other structural parameters, the analysis is still hampered by partial-volume blurring of the trabeculae (100–200 μm thick) with marrow tissue, causing coalescence of the two-peaked intensity histogram (26). Minimum SNR for accurate quantification of bone volume fraction (BVF) has been determined (27) to be ≥ 8, and this in turn limits the minimum voxel size. Hence a factor of 2 SNR gain would allow reduction of the greatest voxel dimension (slice thickness) by one half, thus significantly reducing partial-volume effects and leading to more accurate BVF segmentation.

CONCLUSIONS

The results presented show SNR improvement by a factor of 2.4–3.0 times for in vivo images of the human finger obtained at 1.5 T upon cooling a small, single-loop copper

coil from 300 K to 77 K. In vivo images of the rabbit eye acquired in a similar manner also show SNR gain of about 2. These gains are consistent with a simple model for coil and sample losses and can be predicted from measurements of Q changes upon loading the coil with the sample and upon cooling the coil with the cryogen. While superconducting materials have been shown to permit even higher SNR gains, they usually require lower temperatures for optimum performance at moderate to high field strengths and thus require more complex dewars. The data presented here demonstrate the potential of cryo-cooled conventional metal coils for MR microscopy and suggest applications to a wide range of biomedical imaging problems.

ACKNOWLEDGMENTS

The authors thank Dr. Masaya Takahashi for help with the rabbit imaging and Dr. Tom Connick for helpful discussions.

REFERENCES

1. Callaghan PT. Principles of nuclear magnetic resonance microscopy: Clarendon Press, Oxford; 1991.
2. Styles P, Soffe NF, Scott CA, Cragg DA, Row F, White DJ, White PCJ. A high-resolution NMR probe in which the coil and preamplifier are cooled with liquid helium. J Magn Reson 1984;60:397–404.
3. Hoult DI, Lauterbur PC. The sensitivity of the zeugmatographic experiment involving human samples. J Magn Reson 1979;34:425–433.
4. Hall AS, Barnard B, McArthur P, Gilderdale DJ, Young IR, Bydder GM. Investigation of a whole-body receiver coil operating at liquid nitrogen temperatures. Magn Reson Med 1988;7:230–235.
5. Okada H, Hasegawa T, Heteren JGv, Kaufman L. High temperature superconductor coated RF spine coil for low field MRI. In: Proceedings of the SMR Annual Meeting, San Francisco, 1994. p 223.
6. Heteren JGv, James TW, Bourne LC. Thin film high temperature superconducting RF coils for low field MRI. Magn Reson Med 1994;32:396–400.
7. Vester M, Steinmeyer F, Roas B, Thummes G, Klundt K. High temperature superconducting surface coils with liquid nitrogen or pulse tube refrigeration. In: ISMRM 5th Scientific Meeting and Exhibition, Vancouver, BC, 1997. p 1528.
8. Black RD, Early TA, Roemer PB, Mueller OM, Mogro-Campero A, Turner LG, Johnson GA. A high-temperature superconducting receiver for nuclear magnetic resonance microscopy. Science 1993;259:793–795.
9. Miller JR, Hurlston SE, Ma QY, Face DW, Kountz DJ, MacFall JR, Hedlund LW, Johnson GA. Performance of a high-temperature superconducting probe for in vivo microscopy at 2.0 T. Magn Reson Med 1999;41:72–79.
10. Nyquist H. Thermal agitation of electric charge in conductors. Phys Rev 1928;32:110–113.
11. Jerosch-Herold M, Kirschman RK. Potential benefits of a cryogenically cooled NMR probe for room-temperature samples. J Magn Reson 1989; 85:141–146.
12. Suits BH, Garroway AN, Miller JB. Surface and gradiometer coils near a conducting body: the lift-off effect. J Magn Reson 1998;135:373–379.
13. Lide DR, editor. CRC handbook of chemistry and physics, 75th ed. Boca Raton: CRC Press, Inc.; 1995.
14. Schnall MD, Barlow C, Subramanian VH, Leigh JS. Wireless implanted magnetic resonance probes for in vivo NMR. J Magn Reson 1986;68: 161–167.
15. Song HK, Wehrli FW. Variable TE gradient and spin echo sequences for in vivo MR microscopy of short T2 species. Magn Reson Med 1998;39: 251–258.
16. Wehrli FW, Kanal E. Orbital imaging: factors determining magnetic resonance imaging appearance. Radiol Clin North Am 1987;25:419–427.
17. Odoj F, Rommel E, Kienlin Mv, Haase A. A superconducting probehead applicable for nuclear magnetic resonance microscopy at 7 T. Rev Sci Instrum 1998;69:2708–2712.
18. Banson ML, Cofer GP, Hedlund LW, Johnson GA. Surface coil imaging of rat spine at 7.0 T. Magn Reson Imag 1992;10:929–934.
19. Kolodny NH, Kohler SJ, Rettig ES, Botti PA, D'Amico DJ, Gragoudas ES. A feasibility study of 23Na magnetic resonance imaging of human and rabbit vitreal disorders. Invest Ophthalmol Vis Sci 1993;34:1917–1922.
20. Toussaint J-F, Southern JF, Fuster V, Kantor HL. 13C-NMR spectroscopy of human atherosclerotic lesions. Arterioscler Thromb 1994;14: 1951–1957.
21. Goettmann S, Drape JL, Idy-Peretti I, Bittoun J, Thelen P, Arrive L, Belaich S. Magnetic resonance imaging: a new tool in the diagnosis of tumours of the nail apparatus. Br J Dermatol 1994;130:701–710.
22. Maurer J, Knollmann FD, Schlums D, Garbe C, Vogl TJ, Bier J, Felix R. Role of high-resolution magnetic resonance imaging for differentiating melanin-containing skin tumors. Invest Radiol 1995;30:638–643.
23. Blackband SJ, Charkrabarti I, Gibbs P, Buckley DL, Horsman A. Fingers: Three-dimensional MR imaging and angiography with a local gradient coil. Radiology 1994;190:895–899.
24. Wong EC, Jesmanowicz A, Hyde JS. High-resolution, short echo time MR imaging of the fingers and wrist with a local gradient coil. Radiology 1991;181:393–397.
25. Yuan C, Skinner MP, Kaneko E, Mitsumori LM, Hayes CE, Raines EW, Nelson JA, Ross R. Magnetic resonance imaging to study lesions of atherosclerosis in the hyperlipidemic rabbit aorta. Magn Reson Imag 1996;14:93–102.
26. Wehrli FW, Hwang SN, Ma J, Song HK, Ford JC, Haddad JG. Cancellous bone volume and structure in the forearm: noninvasive assessment with MR microimaging and image processing. Radiology 1998;206: 347–357.
27. Chung H-W, Wehrli FW, Williams JL, Kugelmass SD, Wehrli SL. Quantitative analysis of trabecular microstructure by 400 MHz nuclear magnetic resonance imaging. J Bone Miner Res 1995;10:803–811.